 ©2011 Kvantovaya Elektronika and Turpion Ltd

PACS numbers: 42.81.Wg; 42.81.Pa; 78.20.Ls; 42.79.Hp
DOI: 10.1070/QE2011v041n09ABEH014587

Efficient direct magneto-optical phase modulation of light waves in spun microstructured fibres

V.P. Gubin, S.K. Morshnev, N.I. Starostin, Yu.K. Chamorovsky,
A.I. Sazonov, Ya.V. Przhiyalkovskii, A.I. Boev

***Abstract*. We have proposed a phase modulator of optical radiation for an interferometric electric-current sensor. The modulator takes advantage of the Faraday effect in spun microstructured optical fibres. Such fibres enable small-diameter multiturn fibre coils to be produced, which is necessary for achieving a preset phase modulation amplitude at a moderate drive current. The principal characteristics of the modulator have been studied experimentally: frequency response, magneto-optical sensitivity and output signal contrast. The results demonstrate that the modulator ensures high efficiency, approaching the theoretical one, provided the modulation period exceeds the time it takes light to pass through the fibre. We have examined the influence of spun fibre parameters on the performance of the modulator.**

Keywords: *Faraday effect, optical radiation, spun microstructured fibre, phase modulator.*

1. Introduction

Modulation measurements of the phase shift between waves carrying information about the measurand are widely used in interferometric fibre-optic sensors of physical variables. Such devices include fibre-optic electric-current sensors based on the Faraday effect [1, 2]. The longitudinal magnetic field of the electric current to be measured induces a phase shift between orthogonal circularly polarised light waves in the fibre of the interferometer. The shift is proportional to the current and is measured using an optical interferometer that includes a modulator of the phase difference between the waves. Use is commonly made of piezoelectric modulators, which utilise fibre tension, or electro-optical crystal modulators. A distinctive feature of such modulators is their optical reciprocity, so a delayed modulation method should be used [3]. In addition, a certain optical path length of the interferometer, adjusted to the phase difference modulation frequency, is needed. The method requires a polarisation-maintaining-fibre delay line. It is worth noting that such modulators may generate spurious signals at the modulation frequency [4], which lead to errors in the fibre-optic sensor.

Phase modulation with the use of a nonreciprocal Faraday effect in silica fibre offers the possibility of creating a modulator that would ensure direct (delay-free) modulation of the phase difference between light waves. A key component of fibre-optic Faraday modulators is a fibre coil located inside a toroidal solenoid carrying an electric current. The coil should be made of fibre capable of effectively accumulate the Faraday-effect-induced phase shift along its length.

Such a modulator has a number of useful properties. When it is used in an interferometer, no delay line is needed, and both dc and ac control signals can be employed. In view of this, such modulators can be used to create and adjust a constant phase shift between interfering waves. Their advantage is the possibility of creating an all-fibre optical channel for an electric-current sensor using essentially one type of fibre.

At the same time, because of the low magneto-optical sensitivity of silica, this type of modulator requires a multiturn fibre coil. In particular, to obtain a phase difference modulation amplitude $\varphi_m \sim 2$ rad at a current of ~ 2 A through the plane of a fibre coil, the coil should have of the order of 10^4 turns. This can only be ensured by using a spun microstructured fibre with a small beat length of the built-in linear birefringence, $L_b \sim 1$ mm, which can be wound onto a spool of small radius (down to 2 – 3 mm) almost without optical power losses and, most importantly, without preventing the Faraday-effect-induced phase shift from effectively accumulating along the fibre [5 – 7]. Because spin pitches of the birefringence axes, L_{sp}, less than 2 mm are technically difficult to produce during the fibre drawing process, it is impossible to ensure the relationship $L_b \geqslant L_{sp}$, optimal in terms of magneto-optical sensitivity. As a result, when light propagates along such a fibre, its polarisation state periodically deviates from a circular polarisation [8 – 11], thereby reducing the magnetic field sensitivity of the fibre. At the same time, the high birefringence in the spun microstructured fibres we used compensates in large measure for the unwanted effect of coiling-induced bending strain on the polarisation down to bending radii of ~ 1 mm [11, 12]. Because of this, the Faraday-effect-induced phase shift accumulation effectiveness, even though lower in comparison with an ideal fibre, remains quite sufficient.

Important characteristics of modulators that are used in interferometric sensors are their magneto-optical sensitivity and contrast, which determines the fraction of the total

V.P. Gubin, S.K. Morshnev, N.I. Starostin, Yu.K. Chamorovsky, A.I. Sazonov, Ya.V. Przhiyalkovskii, A.I. Boev V.A. Kotel'nikov Institute of Radio Engineering and Electronics (Fryazino Branch), Russian Academy of Sciences, pl. Vvedenskogo 1, 141190 Fryazino, Moscow region, Russia; e-mail: nis229@ire216.msk.su, yuchamor@gmail.com

Received 14 March 2011; revision received 23 May 2011
Kvantovaya Elektronika **41** (9) 815 – 820 (2011)
Translated by O.M. Tsarev

power of light waves at the modulator input that acquire relative phase modulation. The former characteristic determines the accuracy of the sensor, and the latter determines its threshold sensitivity. In addition, an important characteristic of modulators is the variation of the phase modulation amplitude with modulation frequency (amplitude–frequency response). In particular, it depends on the length of the fibre segment exposed to a magnetic field. This characteristic determines the working modulation frequency band.

The purpose of this work was to theoretically and experimentally study the above characteristics of a Faraday-effect phase modulator based on spun microstructured fibre.

2. Theory

2.1 Operating principle of an ideal modulator

The proposed phase modulator is shown schematically in Fig. 1a. The modulator includes a fibre coil (*1*) located in a toroidal solenoid (*2*), whose turns pass across the plane of the coil. When an electric current flows through the solenoid, the fibre coil is in the longitudinal magnetic field of the current. The modulator under consideration operates in reflection. A polariser (not shown in Fig. 1a) is placed at the input/output of the modulator. The working light waves of the modulator are orthogonal circularly polarised waves. A superposition of such waves forms a linearly polarised wave at the output of the polariser. Light waves are launched into the fibre coil of the modulator, pass through its turns, are reflected by a mirror (*3*), and return along the same path.

The longitudinal magnetic field of the solenoid induces a circular birefringence in the fibre of the modulator. Quasi-circularly (right and left) polarised waves propagate along the coil at different velocities, and the round-trip Faraday-effect-induced phase difference between them is

$$\varphi_F = 4VSN_1N_2I_0, \tag{1}$$

where V (rad A^{-1}) is the Verdet constant of the fibre; $S < 1$ is the relative sensitivity of the fibre; N_1 is the number of turns in the coil; N_2 is the number of turns in the solenoid; and I_0 is the current through the solenoid.

In the absence of any current through the solenoid, the round-trip optical path difference between orthogonally polarised waves in the fibre coil is zero because reflection of circularly polarised waves from the mirror changes their propagation direction and, hence, the waves become orthogonal. As a result, all the phase shifts induced by the intrinsic birefringence of a real fibre are completely compensated for. For this reason, the linearly polarised wave emerging from the polariser returns to it in the same polarisation state as at the input, and the contrast of the modulator is 100 %. The magnetic field generated by a current through the solenoid produces an uncompensated phase shift, φ_F, between circularly polarised waves, which shows up in that the light coming to the polariser is linearly polarised and its plane of polarisation makes an angle $\varphi_F/2$ with that of the input light. It can be shown that, at the output of the modulator, the optical power as a function of the current through the solenoid has the form of an interference pattern:

$$P(I_0) = P_0[1 + K(x)\cos(\varphi_F(I_0))]$$

$$= P_0\{1 + K(x)\cos[4VS(x)N_1N_2I_0]\}. \tag{2}$$

Here $K(x)$ and $S(x)$ are the contrast and sensitivity of the modulator, which depend on a number of parameters (x), and P_0 is the power of the light waves at the input of the modulator. The contrast $K(x)$ characterises the relative power, P_{FM}, of the light waves that acquire phase modulation in the modulator:.

$$K(x) = \frac{P_{FM}}{P_0} = \frac{P_{max} - P_{min}}{P_{max} + P_{min}}. \tag{3}$$

Here P_{max} and P_{min} are the maximum and minimum powers of the light at the output of the polariser, which correspond to phase shifts, φ_F, in (2) of 0 and π, respectively. Note that this definition of the contrast of the wanted signal of a modulator coincides with the visibility factor of the interferometer into which the modulator is incorporated. Generally, the $K(x)$ and $S(x)$ characteristics depend on the amplitude and frequency of the current, parameters of the magnetosensitive fibre, mechanical forces and temperature, and determine the current-sensing performance of the modulator.

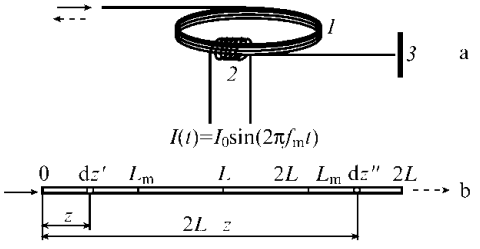

Figure 1. (a) Schematic of the modulator: (*1*) fibre coil, (*2*) solenoid, (*3*) mirror. (b) Equivalent schematic diagram of the fibre coil in the modulator (see text).

2.2 Effect of spun fibre parameters on the performance of the modulator

As pointed out above, the main parameters of high-birefringence spun microstructured fibre that is used in modulators ($L_b \sim 1$ mm, $L_{sp} \sim 2 - 4$ mm) are such that the fibre maintains a circular polarisation of waves only partially. The reason for this is that, at the above parameters, the polarisation state of light periodically deviates from a circular polarisation, and the deviation may be significant (to the point of linear polarisation [6, 7]). Because of this, light waves that propagate along such a spun fibre are most of the time in an elliptic polarisation state, which reduces the Faraday-effect-induced phase shift accumulation effectiveness. The effectiveness can be evaluated using the expression for the magneto-optical sensitivity of a straight spun fibre [11]:

$$S(L_b, L_{sp}) = \frac{2L_b}{\sqrt{4L_b^2 + L_{sp}^2}}, \tag{4}$$

which demonstrates that the sensitivity decreases with decreasing L_b/L_{sp} ratio, as does the contrast of the modulator. Indeed, orthogonally polarised waves propagat-

ing along a spun fibre may experience changes in their ellipticity, rotation direction and azimuth angle, remaining nevertheless orthogonal. After passing a segment of the fibre of length z, the waves have an unwanted phase difference proportional to the fibre length, which can be compensated in reflection mode. As pointed out above, this can be achieved with a mirror that causes waves to propagate along the same portion of the fibre in the opposite direction and changes their polarisation state to the orthogonal one (a right-hand elliptical polarisation should convert to a left-hand one and vice versa). Unfortunately, an elliptically polarised wave cannot be converted to an orthogonally polarised one by a Fresnel reflector or metallic mirror [13]. As a result, after a round trip through the fibre coil, waves capable of interfering will have a smaller amplitude at the input/output of the modulator in comparison with the case when circularly polarised waves are incident on a mirror. Accordingly, the contrast decreases.

Let us show this in a more rigorous way. The Jones vector of a wave with an arbitrary elliptical polarisation U, ellipticity angle ε and azimuth angle θ has the form [13]

$$\left|\begin{matrix}E_X\\E_Y\end{matrix}\right|_U = A\exp(\mathrm{i}\delta)\left|\begin{matrix}\cos\theta\cos\varepsilon - \mathrm{i}\sin\theta\sin\varepsilon\\ \sin\theta\cos\varepsilon + \mathrm{i}\cos\theta\sin\varepsilon\end{matrix}\right|. \tag{5}$$

Here δ is the initial phase, the same for E_x and E_y. The orthogonal polarisation state W can be obtained through the substitutions $\theta \to \theta \pm \pi/2$ and $\varepsilon \to -\varepsilon$:

$$\left|\begin{matrix}E_X\\E_Y\end{matrix}\right|_W = A\exp(\mathrm{i}\delta)\left|\begin{matrix}-\sin\theta\cos\varepsilon + \mathrm{i}\cos\theta\sin\varepsilon\\ \cos\theta\cos\varepsilon + \mathrm{i}\sin\theta\sin\varepsilon\end{matrix}\right|. \tag{6}$$

After the reflection of wave U from a mirror, the resultant wave will be represented by the Jones vector

$$\left|\begin{matrix}E'_X\\E'_Y\end{matrix}\right|_U = A\exp(\mathrm{i}\delta)\left|\begin{matrix}-\cos\theta\cos\varepsilon + \mathrm{i}\sin\theta\sin\varepsilon\\ \sin\theta\cos\varepsilon + \mathrm{i}\cos\theta\sin\varepsilon\end{matrix}\right|. \tag{7}$$

The polarisation of the reflected wave can be expressed through the orthogonal polarisations U and W [see (5) and (6)]:

$$\left|\begin{matrix}E'_X\\E'_Y\end{matrix}\right|_U = a_U\left|\begin{matrix}E_X\\E_Y\end{matrix}\right|_U + b_U\left|\begin{matrix}E_X\\E_Y\end{matrix}\right|_W. \tag{8}$$

Substituting the Jones vectors (5)–(7) into (8), we find the coefficients a_U and b_U:

$$\begin{aligned} a_U &= -\cos 2\theta\cos 2\varepsilon,\\ b_U &= \sin 2\theta + \mathrm{i}\cos 2\theta\sin 2\varepsilon. \end{aligned} \tag{9}$$

The absolute squares of these coefficients have a clear physical meaning: $|a_U|^2$ is the relative power of a wave that had polarisation U both before and after reflection from the mirror, and $|b_U|^2$ is the relative power of a wave that had polarisation U before reflection and polarisation W after:

$$\begin{aligned} |a_U|^2 &= \cos^2 2\theta\cos^2 2\varepsilon,\\ |b_U|^2 &= \sin^2 2\theta + \cos^2 2\theta\sin^2 2\varepsilon. \end{aligned} \tag{10}$$

It is easy to see that $|a_U|^2 + |b_U|^2 = 1$. During the propagation through the spun fibre in the reverse direction, the wave with polarisation W will compensate for the phase delay accumulated during the propagation in the forward direction, whereas the phase delay of the wave with polarisation U will continue to increase.

It is easy to show that the coefficients in the representation of the reflected wave W in terms of polarisations U and W are given by

$$\begin{aligned} a_W &= \cos 2\theta\cos 2\varepsilon,\\ b_W &= \sin 2\theta - \mathrm{i}\cos 2\theta\sin 2\varepsilon. \end{aligned} \tag{11}$$

It is seen that $b_W = b_U^*$ and that the absolute squares of the coefficients a_W and b_W are identical to (10). It should be emphasised that $|a_W|^2$ is the relative power of the wave that had polarisation W both before and after reflection from the mirror, and $|b_W|^2$ is the relative power of the wave that had polarisation W before reflection and polarisation U after.

Only waves that have compensated the phase shift will be able to interfere at the detector, and the interference term will be proportional to $b_U b_W$:

$$\begin{aligned} b_U b_W &= \sin^2 2\theta + \cos^2 2\theta\sin^2 2\varepsilon\\ &= \sin^2 2\varepsilon + \sin^2 2\theta\cos^2 2\varepsilon. \end{aligned} \tag{12}$$

When a mirror reflects waves whose polarisation states are close to a right- or left-hand circularly polarised state ($\varepsilon \approx \pi/4$), we have $b_U b_W \approx 1$, and the interference pattern has the maximum visibility. For the reflection of almost linearly polarised waves ($\varepsilon \approx 0$), we have $b_U b_W \approx \sin^2 2\theta$, i.e. this product depends on the azimuth angle θ. In intermediate instances, the visibility of the interference pattern depends on both θ and ε.

The above analysis is valid for monochromatic light. In the case of a wide spectrum, elliptically polarised waves incident on the mirror have various azimuth angles in a range considerably broader than 2π. Averaging relation (12) over the entire θ range, we find the visibility of the interference pattern for a wide spectrum:

$$K(\varepsilon) = \langle b_U b_W\rangle = \sin^2 2\varepsilon. \tag{13}$$

To evaluate the contrast, we can use an average ellipticity angle of the light polarisation in a spun fibre:

$$2\varepsilon_0 = \arcsin\left(1 - \frac{L_{\mathrm{sp}}^2}{L_{\mathrm{sp}}^2 + 4L_{\mathrm{b}}^2}\right). \tag{14}$$

Substituting (14) into (13), we obtain

$$K(\varepsilon_0) \simeq \left(\frac{4L_{\mathrm{b}}^2}{L_{\mathrm{sp}}^2 + 4L_{\mathrm{b}}^2}\right)^2. \tag{15}$$

It follows from (15) that the contrast should decrease markedly with decreasing $L_{\mathrm{b}}/L_{\mathrm{sp}}$ ratio.

2.3 Frequency characteristic of modulator sensitivity

The Faraday effect has a very fast response. The decrease in modulation efficiency with increasing modulation frequency is due to the fact that the modulation period becomes comparable to the time it takes light to pass through the fibre-optic section of the modulator. Let us derive relations

for the amplitude and initial phase of the Faraday-effect-induced phase shift at the output of a modulator for a sinusoidal current through the solenoid of the modulator: $I_0(t) = I_{0m} \sin(2\pi f_m t)$. We make the following assumptions: The fibre of the modulator is taken to transmit waves of any polarisation with no distortion (an ideal fibre for the Faraday effect) and to be characterised only by the refractive index of silica, which determines the speed of light in the fibre. In addition, the ac magnetic field is taken to be uniform along the entire fibre in the coil, meaning that the initial phase of the field is the same throughout the fibre.

Consider the equivalent schematic diagram of the fibre section of the modulator in Fig. 1b. The fibre segment between zero and L_m is exposed to a magnetic field (the total fibre length, L, includes the output portion of the fibre, which is in zero magnetic field). A round trip of light in a real modulator in the model under consideration is taken into account by adding a length L of the fibre. Its portion from $2L - L_m$ to $2L$ is exposed to a magnetic field (Fig. 1b). Note that, to adequately evaluate the Faraday-effect-induced phase shift in this model, the magnetic field direction should be the same for the two sections of the fibre. Phase shifts are then summed up, like in a real modulator. In this model, the Faraday-effect-induced phase shift in an element dz of the fibre (Fig. 1b) can be written in the form

$$d\varphi_F(z) = 2VI(z,t)dz/(\pi R), \tag{16}$$

where R is the radius of the fibre coil. At the instant in time when the light wave passes through the element dz, the current is

$$I(z,t) = I_0[\sin(2\pi f_m t - 2\pi f_m z n/c)], \tag{17}$$

where n is the refractive index of silica and c is the speed of light. Substituting (17) into (16) and integrating over the ranges $0 \leqslant z \leqslant L_m$ and $2L \geqslant z \geqslant 2L - L_m$, we obtain the following relation for the total phase shift in the coil of the modulator:

$$\varphi_F(f_m) = A(f_m)\sin[2\pi f_m t + \psi(f_m)], \tag{18}$$

where the amplitude and initial phase are given by

$$\frac{A(f_m)}{A(0)} = \frac{\sin(\pi f_m n L_m/c)\cos[(\pi f_m n/c)(2L - L_m)]}{\pi f_m n L_m/c}, \tag{19}$$

$$A(0) = \frac{2VI_0L_m}{\pi R}, \tag{20}$$

$$\psi(f_m) = 2\pi f_m nL/c. \tag{21}$$

Relation (19) is the frequency characteristic of the modulator sensitivity normalised to the zero-frequency sensitivity. The latter is given by relation (20), which indicates that, at zero frequency, the modulator introduces an expected constant phase sift $\varphi_F(0) = A(0) = 4VI_0N$, where $N = L_m(2\pi R)^{-1}$ is the number of turns in the fibre coil.

3. Experimental

For experimental studies, the modulator was incorporated into a linear reflective interferometer, schematised in Fig. 2. The interferometer included a light source (*1*), directional coupler (*2*), polariser (*3*), mirror (*8*) and a modulator in the form of a fibre coil (*5*) situated inside a toroidal solenoid (*6*). The fibre segments (*4*) and (*7*), located outside the magnetic field of the solenoid, connected the modulator to the optical system of the interferometer. The reflected light was detected by a photodiode (*9*) placed at the coupler output. The signal from the photodiode was fed to an oscilloscope (*10*).

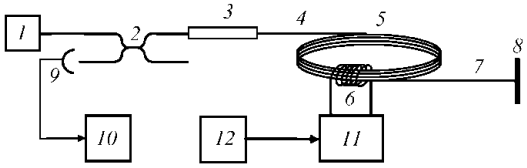

Figure 2. Schematic of the experimental setup: (*1*) light source, (*2*) directional coupler, (*3*) polariser, (*4*) input end, (*5*) modulator coil, (*6*) solenoid, (*7*) output end, (*8*) mirror, (*9*) photodiode, (*10*) oscilloscope, (*11*) current amplifier, (*12*) generator.

In our experiments, the toroidal solenoid was powered by an alternating or direct current. Frequency characteristics were measured using a standard sine wave generator (*12*), which ensured a current of 600 mA at frequencies from 20 Hz to 100 kHz. Electric-current sensors typically employ harmonic phase modulation with an amplitude of ~ 2 rad, ensured by a current of several amperes, which is produced by a current amplifier (*11*) with a 40-kHz resonance circuit.

The light source used was an erbium-doped fibre oscillator (wavelength, 1.55 μm) with a 30-mW output power and 25-nm emission bandwidth. The multiturn coil of the modulator was made of a spun microstructured fibre which had a quasi-elliptical silica core surrounded by six air holes.

In our studies, we used two types of spun microstructured fibres, with $L_b = 5$ mm and $L_{sp} = 3.5$ mm (type I) or $L_b = 1$ mm and $L_{sp} = 4$ mm (type II). The modulator coil of the type I fibre had $N_1 = 10^4$ turns around a silica tube 20 mm in outer diameter and 100 mm in length. The toroidal solenoid, which generated a longitudinal magnetic field in the fibre of the modulator, had $N_2 = 48$ turns of 1.2-mm-diameter copper wire. The wire turns passed through the inner hole of the silica tube and covered it on the outside to form a toroidal solenoid. The fibre segment (*7*), located outside the magnetic field, had a length $L_0 = 200$ m and was wound onto a spool of diameter 30 mm. The total length of the spun microstructured fibre in the interferometer was 900 m, and the optical loss was ~ 3 dB.

The modulator coil of the type II fibre had $N_1 = 8500$ turns around a silica tube 12 mm in outer diameter and 100 mm in length. The toroidal solenoid had $N_2 = 47$ turns of 0.9-mm-diameter copper wire. The total length of the spun microstructured fibre in the interferometer was 400 m, and the optical loss was within 5 dB.

Figure 3 shows the relative optical power at the photodetector input as a function of the dc current through the solenoid for the two types of fibres in the modulator coil [the filled and open squares represent experimental data for the type I and II spun fibres, and the curves represent the best fit to Eqn (2)]. It follows from Fig. 3 that the relative magneto-

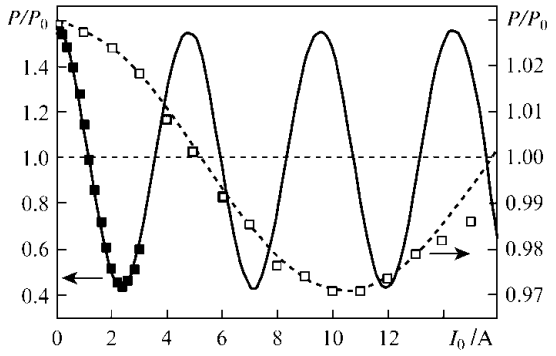

Figure 3. Relative optical power measured at the photodetector input as a function of the dc current through the solenoid: $L_b = 5$ mm, $L_{sp} = 3.5$ mm (filled squares); $L_b = 1$ mm, $L_{sp} = 4$ mm (open squares). The curves show fits with cosine functions.

optical sensitivity of the type I and II spun fibre coils is $S = 0.97$ and 0.265, respectively. The contrast, K, of the output signal for these fibres is 0.56 and 0.029.

We measured the amplitude–frequency response of a modulator fabricated using the type I spun fibre, with a beat length $L_b = 5$ mm. The magnetic-field-induced modulation of the phase shift between optical modes showed up as a periodic modulation of the optical power at the interferometer output:

$$P(t) = P_0\{1 + K\cos[\varphi_F(f_m)\sin(2\pi f_m t)]\}. \quad (22)$$

Here $\varphi_F(f_m) = 4VSN_1N_2I_0[A(f_m)/A(0)]$ is the modulation amplitude of the Faraday-effect-induced phase shift, which depends on modulation frequency as represented by Eqn (19). Intensity (22) comprises a constant component and a time-dependent (modulation) component. At a small modulation amplitude, the modulation component of the intensity is

$$P_m(t) \approx \tfrac{1}{2}P_{m0}(f_m)\cos(4\pi f_m t), \quad (23)$$

where $P_{m0}(f_m) = P_0K[\varphi_F(f_m)]^2$ is the peak-to-peak amplitude of the modulation component.

Therefore,

$$\varphi_F(f_m) = \left[\frac{P_{m0}(f_m)}{P_0K}\right]^{1/2} = \text{const}\,[P_{m0}(f_m)]^{1/2}. \quad (24)$$

Relation (24) was relied on in developing a technique for measuring the frequency response of modulator sensitivity. $P_{m0}(f_m)$ was measured using an oscilloscope. The peak-to-peak intensity modulation amplitude was measured at a constant current through the solenoid: $I_0 = 600$ mA. The normalised measured frequency response is shown in Fig. 4 together with a fit to relation (19).

In addition, our experiments showed that the modulator under examination was free of spurious signals such as concomitant intensity modulation, typical of modulators based on piezoelectric or electro-optical delayed modulation [4].

4. Analysis of the results

This paper examined the frequency response of a Faraday-effect phase modulator and the influence of spun fibre parameters on the sensitivity and contrast of the modulator.

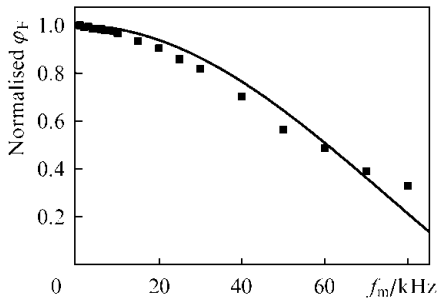

Figure 4. Frequency response of a Faraday modulator (the solid squares represent the experimental data and the curve shows a theoretical fit).

Comparison of the calculated frequency characteristics of the modulator to experimental data (Fig. 4) demonstrates satisfactory agreement at low frequencies, where the modulation period exceeds the time it takes light to pass through the fibre. The discrepancy at higher frequencies may be the result of the averaging of the oscillating Faraday-effect-induced phase shift, in particular because the current-carrying solenoid is also a distributed element, which was left out of consideration in the above theory.

Analysis of the frequency response (19) indicates that the use of a Faraday modulator in an interferometer limits the total fibre length. The nonreciprocity of the modulator makes the use of a delay line, necessary in systems with reciprocal modulators, unnecessary or even detrimental.

Consider now the influence of fibre parameters on the sensitivity (scale factor) and contrast of the modulator. On the one hand, to achieve high sensitivity and contrast the condition $L_{sp}/L_b < 1$ should be met, which allows waves propagating through the fibre to remain almost circularly polarised [7, 8]. On the other hand, L_b should be small compared to the beat length of the birefringence (L_{ind}) induced by various deformations of the fibre, primarily by small-radius coiling ($R \leqslant 1$ cm). However, for the former condition to be met, too small a spin pitch will then be necessary, unachievable at present for technical reasons. Thus, a trade-off between these fibre parameters is needed.

To analyse the sensitivity of spun fibre, we used relation (4). Figure 5 shows calculated $S(L_b)$ for two spin pitches corresponding to our experiments [curves (*1*) and (*2*) for

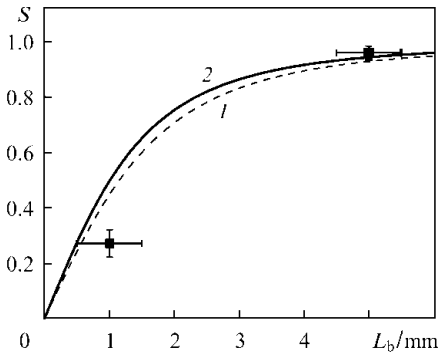

Figure 5. Relative sensitivity of the modulator as a function of the built-in birefringence beat length for spun fibres with spin pitches $L_{sp} =$ (*1*) 4 and (*2*) 3.5 mm (calculation). The filled squares represent experimental data for $L_b = 1$ mm, $L_{sp} = 4$ mm and $L_b = 5$ mm, $L_{sp} = 3.5$ mm.

$L_{sp} = 4$ and 3.5 mm, respectively]. The experimental data are represented by filled squares. It follows from Fig. 5 that the experimental data agree well with theoretical predictions [6–8].

To analyse the contrast of the output signal of the spun fibre modulator in an interferometer, we used relation (15). Figure 6 shows calculated $K(L_b)$ for two spin pitches [curves (*1*) and (*2*) for $L_{sp} = 4$ and 3.5 mm, respectively]. The experimental data are represented by filled squares. The reduction in contrast with decreasing L_b can be accounted for by the deviation of the polarisation states of the optical modes from a circular polarisation, which decreases the fraction of light involved in interference after the reflection from the mirror [see (13)]. The discrepancy between the theoretical prediction and experimental point for the type I fibre may result from the influence of the fibre segment between the coil and mirror on the contrast.

The present experimental and theoretical results can be used to select parameters of spun microstructured fibres for modulator coils.

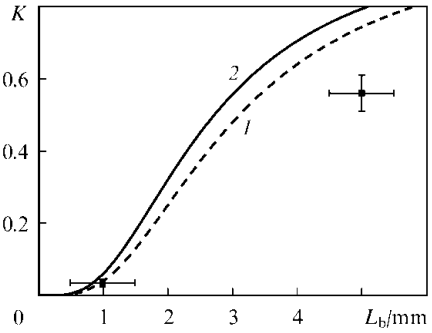

Figure 6. Contrast of the modulator signal as a function of the built-in birefringence beat length for spun fibres at a constant spin pitch (the curves show calculation results and the filled squares represent experimental data). The parameters of the modulator are the same as in Fig. 5.

5. Conclusions

We have proposed an efficient phase modulator based on a nonreciprocal Faraday effect in spun microstructured optical fibres. Such fibres retain their magneto-optical sensitivity even at small bending radii and enable multiturn coils to be produced in order to achieve the required phase modulation amplitude (several radians). The proposed modulator is intended for use in interferometric electric-current sensors. Its distinctive feature is direct (delay-free) modulation, which requires no delay line. We have studied the amplitude–frequency response of the Faraday modulator in the range 0–80 kHz. The results demonstrate that the modulator ensures high efficiency, approaching the theoretical one, provided the modulation period exceeds the time it takes light to pass through the fibre. Experimental data show that the modulator is free of spurious signals at the modulation frequency. We have examined the influence of spun fibre parameters on the magneto-optical sensitivity of the modulator and the contrast of its output signal in a reflective interferometer with the aim of optimising fibre parameters. The proposed phase modulator offers the possibility of implementing a new optical scheme of an electric-current sensor using one type of fibre: spun microstructured fibre.

References

1. Enokihara A., Isutsu M., Sueta T. *J. Lightwave Technol.*, **5**, 1584 (1987).
2. Bohnert K., Gabus P., Nehring J., Brandle H. *J. Lightwave Technol.*, **20**, 267 (2002).
3. Kintner E.C. *Opt. Lett.*, **6**, 154 (1981).
4. Szafraniec B., Blake J. *J. Lightwave Technol.*, **12**, 1679 (1994).
5. Chamorovskiy Yu.K., Starostin N.I., Ryabko M.V., Sazonov A.I., Morshnev S.K., Gubin V.P., Vorob'ev I.L., Nikitov S.A. *Opt. Commun.*, **282**, 4618 (2009).
6. Chamorovsky Yu.K., Starostin N.I., Morshnev S.K., Gubin V.P., Ryabko M.V., et al. *Kvantovaya Elektron.*, **39**, 1074 (2009) [*Quantum Electron.*, **39**, 1074 (2009)].
7. Chamorovsky Yu.K., Starostin N.I., Ryabko M.V., et al. *Opt. Mem. Neural Networks*, **18**, 278 (2009).
8. Polynkin P., Blake J. *J. Lightwave Technol.*, **23**, 3815 (2005).
9. Michie A., Canning J., Bassett I., et al. *Opt. Express*, **15**, 1811 (2007).
10. Gubin V.P., Morshnev S.K., Starostin N.I., Sazonov A.I., et al. *Radiotekh. Elektron.*, **53**, 971 (2008).
11. Gubin V.P., Isaev V.A., Morshnev S.K., Sazonov A.I., Starostin N.I., et al. *Kvantovaya Elektron.*, **36**, 287 (2006) [*Quantum Electron.*, **36**, 287 (2006)].
12. Morshnev S.K., Gubin V.P., Vorob'ev I.L., Starostin N.I., Sazonov A.I., et al. *Kvantovaya Elektron.*, **39**, 287 (2009) [*Quantum Electron.*, **39**, 287 (2009)].
13. Azzam R.M.A., Bashara N.M. *Ellipsometry and Polarized Light* (Amsterdam–New York–Oxford: North-Holland Publ. Comp., 1977).